

Proceeding Paper

# Modal Shape Visualization Employing FP + 2D-DIC and Phased-Based Motion Magnification <sup>†</sup>

Manuel Pastor-Cintas <sup>1</sup>, Luis Felipe-Sesé <sup>1,\*</sup> , Ángel Molina-Viedma <sup>1</sup> , Elías López-Alba <sup>2</sup>  
and Francisco Díaz-Garrido <sup>2</sup>

<sup>1</sup> Departamento de Ingeniería Mecánica y Minera, EPS Linares, Universidad de Jaén, 23700 Linares, Spain

<sup>2</sup> Departamento de Ingeniería Mecánica y Minera, EPS Jaén, Universidad de Jaén, 23071 Jaen, Spain

\* Correspondence: lfelipe@ujaen.es

<sup>†</sup> Presented at 19th International Conference on Experimental Mechanics, Kraków, Poland, 17–21 July 2022.

**Abstract:** Recently, the combination of Fringe Projection (FP) and 2D Digital Image Correlation (2D-DIC) has become a low-cost alternative for measuring deformations even in dynamic events such as vibration testing. FP and DIC are displacement measurement techniques, so high frequency vibration tests associated with low levels of displacement suppose a challenge. By means of Phase-Based Motion Magnification algorithm (PBMM), the periodic displacement observed in an image sequence can be magnified. This makes it possible to measure clear displacement maps by FP + 2D-DIC even when subtle displacement occurs. This methodology allows a better interpretation of the vibration behavior of mechanical components. In this work, the behavior of a beam excited at its natural frequencies has been studied, showing the potential of PBMM and FP + 2D-DIC

**Keywords:** Fringe Projection; high speed digital image correlation; Motion Magnification



**Citation:** Pastor-Cintas, M.; Felipe-Sesé, L.; Molina-Viedma, Á.; López-Alba, E.; Díaz-Garrido, F. Modal Shape Visualization Employing FP + 2D-DIC and Phased-Based Motion Magnification. *Phys. Sci. Forum* **2022**, *4*, 14. <https://doi.org/10.3390/psf2022004014>

Academic Editors: Zbigniew L. Kowalewski and Elżbieta Pieczyskasz

Published: 5 August 2022

**Publisher's Note:** MDPI stays neutral with regard to jurisdictional claims in published maps and institutional affiliations.



**Copyright:** © 2022 by the authors. Licensee MDPI, Basel, Switzerland. This article is an open access article distributed under the terms and conditions of the Creative Commons Attribution (CC BY) license (<https://creativecommons.org/licenses/by/4.0/>).

## 1. Introduction

The application of full-field optical techniques in experimental mechanics has increased considerably in recent years thanks to the improvement of optical technologies and image processing. One of the most employed techniques is 2D or 3D digital image correlation (DIC) [1], which obtains the displacements in- or out-of- plane respectively. Fringe projection (FP) is other established optical technique, which measures 3D shape maps [2]. Especially important are their possibilities in dynamic testing, such as vibration and impact analysis. Full-field results from these optical techniques have been employed to improve, for example, component life and FEM model updating or analyze the actual behaviour of components, among others [3–12]. 2D-DIC requires only one camera to obtain in-plane measurements ( $-x$ ,  $-y$ ). Moreover, 3D-DIC additionally measures in  $-z$  direction for which a stereoscopic camera system is required. This entails an important increment in versatility but also in the complexity and the economic aspects of the experimental setup.

Recently, the combination of Fringe Projection (FP) and Digital Image Correlation (2D-DIC) has been presented as an alternative to 3D-DIC [13,14]. In fact, it has been applied to different mechanical analyses such as vibration at low excitation frequency [15] or Finite Element Method (FEM) model validation [16]. This technique allows the measurement of 3D displacement maps using a single camera, simplifying the setup and reducing the cost.

FP + 2D-DIC requires a red speckle pattern on the specimen surface and a blue fringe pattern projected on the same surface. Both patterns can be separated using Color Encoding [17] and can be analyzed independently using FP and 2D-DIC algorithms. However, this separation usually leads to some pattern crosstalk. This, together with the fact that FP and 2D-DIC are displacement measurement techniques, means that noisy displacement maps could be obtained when small displacements occur. This is common, for instance, in vibration testing at high excitation frequencies. In this work, a novel tool to improve the

obtaining of clear displacement maps has been explored together with FP + 2D-DIC. This methodology is Phase-Base Motion Magnification (PBMM). It consists of the enhancement of the subtle movement registered in a sequence by decomposing the images into complex steerable pyramid filters and magnifying a specific frequency band [18]. The combination of PBMM and 3D-DIC has been previously evaluated by the authors [19], concluding that Motion Magnification helps to reveal low-amplitude Operational Deflection Shapes (ODSs) using 3D-DIC. A cantilever beam was used to validate the method, comparing the results obtained by 3D-DIC and magnification with numerical models. Once the validation was performed, an industrial object was tested, obtaining the three-dimensional displacements that occurred during excitation.

Hence, with adequate magnification, FP + 2D-DIC could improve its results, increase its versatility and facilitate the interpretation of the modal shapes or ODSs. In fact, in this study, the FP + 2D-DIC and Phase Based Motion Magnification (PMM) integration was explored for the measurement of subtle 3D displacement maps. Firstly, a solid-rigid test was carried out to validate the combination of these methods. Then, a cantilever beam was employed in order to demonstrate the correct performing obtaining ODSs.

## 2. Theoretical Background

### 2.1. FP + 2D-DIC Technique

2D-DIC allows the measurement of in-plane displacements with only one camera. To perform Digital Image Correlation, the surface of the sample has to be previously prepared by spraying it with a random pattern resulting in a speckle pattern. This will facilitate the tracking of sectors of the image (facets) in the different images captured along the process [20]. In fact, DIC requires an image of the sample in a reference state and an image for each state to be studied. The area of interest is divided into virtual facets and the algorithm will associate a measure point to each of them. The correlation of each facet, comparing each image with the reference one, will allow the obtaining of the displacement maps. The displacement measured will be in pixel units, and by using the lateral magnification of the camera-lenses system the displacements in length units can be calculated.

On the other hand, FP is also a full-field optical technique but it measures 3D shapes. Hence, it can be used to determine displacements in the direction of the camera's optical axis. It requires the projection of a pattern of vertical fringes on the sample. Actually it has to be obliquely projected with a certain angle ( $\alpha$ ) with respect to the optical axis of the camera (OA) as shown in Figure 1 [2,21–23]. In order to perform FP, it is necessary to capture a reference image of a flat surface, and then an image is captured for each state of deformation. As the surface deforms, the projected fringes will proportionally deform, which results in a phase shift of these fringes. This effect can be measured using Fourier Transform methodology [2] followed by an unwrapping of the measured phase [23]. To obtain out-of-plane displacements, it is necessary to know the relationship between displacements ( $\Delta z$ ) and the phase of the corresponding displaced fringe ( $\Delta\phi$ ), for which a calibration procedure is required [24].

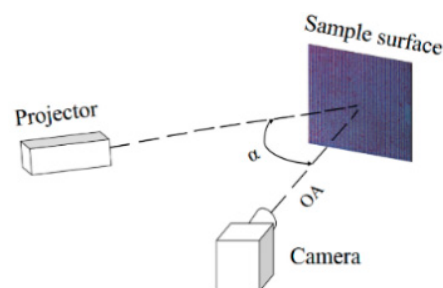


Figure 1. Scheme of FP + 2D-DIC technique.

To sum up, when the surface is deformed, both the speckle and the fringes move together and must be present to be able to process DIC and FP respectively, but they cannot interfere with the corresponding processing algorithms. To overcome that issue, the previously proposed method uses a color Liquid Crystal Display (LCD) projector and an RGB camera [13]. In fact, the projector creates a pattern of blue fringes on a white background with a sinusoidal intensity profile on the measurement surface. This enables FP analysis to be performed in the red spectrum of the images. On the other hand, the background of the sample is painted white and sprayed with red speckle to perform 2D-DIC analysis on the blue image [15].

As previously mentioned, the displacements in  $-x$  and  $-y$  directions measured directly using 2D-DIC are distorted by the shape or deformations in the  $-z$  direction experienced by the element studied during the test [13]. This is because the lateral magnification varies with the distance of the point measured with respect to the camera sensor. For this reason, in-plane displacements require a correction. Authors developed a methodology to perform the correction from the  $-z$  displacements measured by FP [13]. This correction methodology is based on a pin-hole lens model. In this way it is possible to relate the correct displacements in the plane ( $\Delta x$  and  $\Delta y$ ) with the directly measured by 2D-DIC ( $\Delta x_{\text{CCD}}$ ,  $\Delta y_{\text{CCD}}$ ) and the displacements measured out of the plane ( $\Delta z$ ) by means of fringe projection:

$$\begin{aligned} \Delta x &= L \left[ \Delta x_{\text{CCD}} - \left( x_{2,\text{CCD}} \frac{\Delta z_2}{z_0} - x_{1,\text{CCD}} \frac{\Delta z_1}{z_0} \right) \right] \\ \Delta y &= L \left[ \Delta y_{\text{CCD}} - \left( y_{2,\text{CCD}} \frac{\Delta z_2}{z_0} - y_{1,\text{CCD}} \frac{\Delta z_1}{z_0} \right) \right] \end{aligned} \quad (1)$$

where  $(x_{1,\text{CCD}}, y_{1,\text{CCD}})$  and  $(x_{2,\text{CCD}}, y_{2,\text{CCD}})$  are the initial and final positions of pixels displaced from the sample surface,  $\Delta z_1$  and  $\Delta z_2$  are the corresponding out-plane displacements of that pixel,  $z_0$  is the distance between the reference surface and the optical center of the camera lens and  $L$  is the inverse of the lateral magnification in mm/pixel at a distance  $z_0$  [15,24].

## 2.2. Phase Motion Magnification

In this study, the magnification of the displacement observed in the captured images was performed using the Phase-Based Motion Magnification Method (PBMM), developed by Wadhwa et al. [12]. Through this methodology, the image sequence is decomposed into pyramidal descriptors. The temporal variation of the local phase is considered as an indicator of movement. By analyzing the phase signal in the frequency domain, a magnification factor is applied to a desired frequency band. The reconstruction of the sequence considering the modified phase signal provides an amplified version with reduced noise and computational cost. Consequently, magnification requires three parameters: frames per second of the image sequence (frame rate), frequency range to be magnified, and magnification factor ( $M$ ) [12]. Therefore, an amplified version of the images with the band magnified by  $(1 + M)$  is obtained by means of transforming the phase signal back to the time-domain and recomposing the images from the pyramid's filters. Moreover, in order to increase the signal to noise ratio an amplitude-weighted spatial smoothing is applied.

## 3. Materials and Methods

As mentioned, this study aims to validate and show the potential of the integration of FP + 2D-DIC with PBMM. To perform the validation, a rigid body motion test was performed. Additionally, the potential of the integration is presented through vibration tests on a cantilever beam. In this last kind of test, the Operational Deflection Shapes associated to the different natural frequencies are analyzed. The optical system for both cases consists of a camera (JAI Yokohama, Japan AT-200GE, 25 mm lens,  $1624 \times 1236$  pixel) and a projector (EPSON EB W32, Suwa, Japan). The captured RGB images were separated into their RGB channels to process independently speckle and fringe patterns. The data in blue containing the speckles are processed using a commercial digital image correlation algorithm (VIC 2D from Correlated Solutions Inc., Irmo, SC, USA) and the data in red containing the fringes

was processed by a fringe projection algorithm using Fourier transform profilometry and quality guided unwrapping algorithm.

### 3.1. FP + 2D-DIC and PMM Validation Test

A rigid body motion test was performed to validate that the FP + 2-DIC technique together with the PBMM methodology presented logical results. This was executed by analyzing a constrained rigid solid sinusoidal displacement test in a plate where only displacement in the  $-z$  direction occurs. In this way, after performing PBMM separately to speckle and fringe images, processing each set of images using their corresponding algorithms and performing the correction of in-plane displacement, the displacements maps for the  $-x$  and  $-y$  directions should remain negligible. Specifically, a rigid flat plate was employed as shown in Figure 2. A 5 Hz sinusoidal excitation was applied to the shaker while images were acquired at an alias frequency of 0.1 Hz. Subsequently, a  $1.5\times$  magnification factor was used to the set of images. The results of this validation are analyzed in the next section.

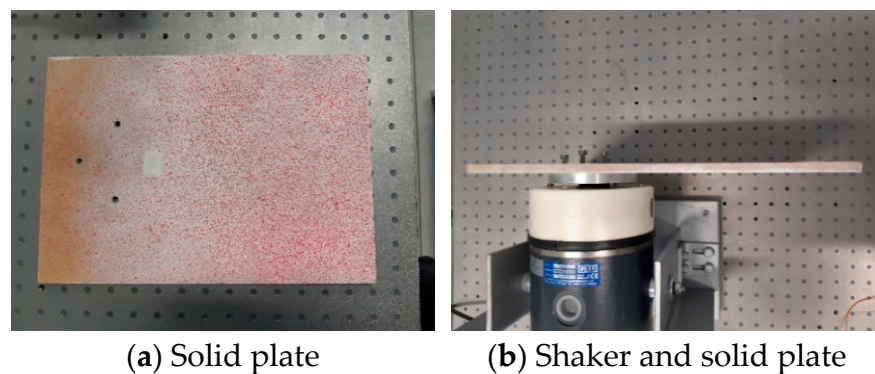


**Figure 2.** Rigid solid and shaker system.

### 3.2. Operational Deflection Shapes Test

Once the validation process was successful, the test was performed on a cantilever beam. A polycarbonate beam with dimensions 160 mm in length, 40 mm in width, and 2 mm in thickness excited with a shaker was tested. In a first step, the natural frequencies were determined by coupling an accelerometer to the beam. Figure 3 shows the layout of the test. The frequency range of interest was up to 600 Hz. The registration of the accelerometer signal and the calculation of the transmissibility function were performed using the real time analyzer Brüel & Kjær, Nærum Denmark, RT Pro software and the controller Brüel & Kjær Photon+. This system also generated the random signal to excite the specimen through the shaker. The natural frequencies obtained are shown in Table 1.

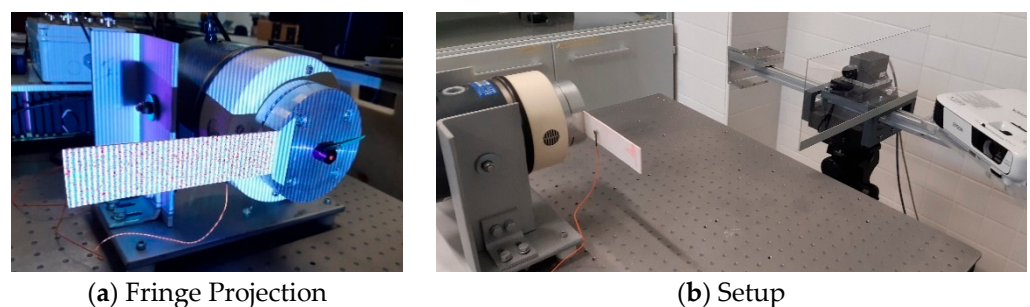


**Figure 3.** ODS test setup.

**Table 1.** Natural frequencies.

Mode	Frequency (Hz)
1	20
2	160
3	440

Afterwards, the behavior of the beam was studied when it was subjected to sinusoidal excitation at specific frequencies, specifically those corresponding to the three resonance frequencies observed in Table 1. The camera frame rate was 4.938, 4.992, and 4.994 Hz entailing 0.246, 0.249, and 0.501 Hz alias frequency respectively for each vibration mode, obtaining a stroboscopic effect. Finally, a 5× magnification factor was applied to speckle and fringe pattern images.

**4. Results**

*4.1. FP + 2D-DIC and PMMM Validation Test*

In-plane displacements maps obtained before ((a) and (b)) and after correction ((c) and (d)) for a maximum deformation are presented in Figure 4.

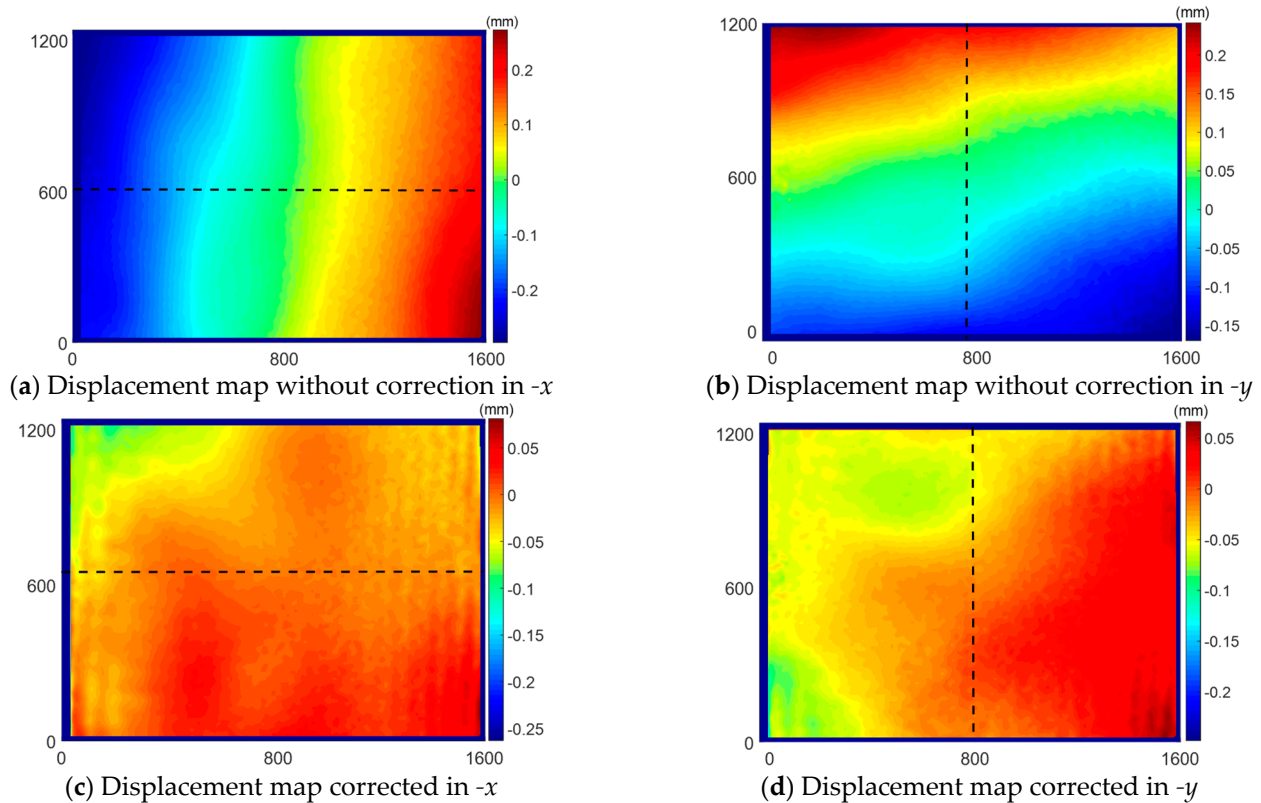
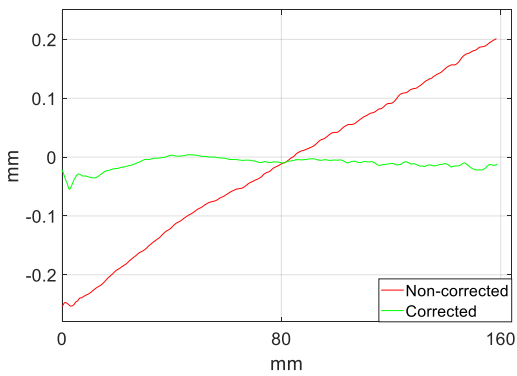
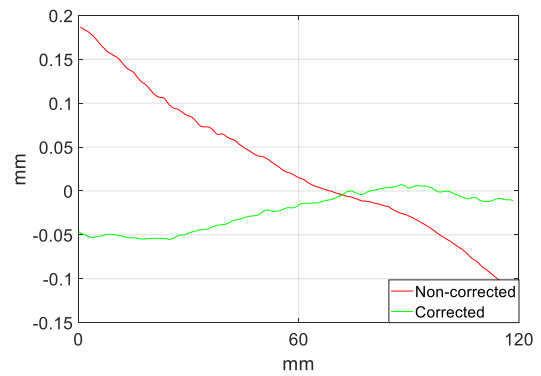


**Figure 4.** Displacement maps in-plane without correction (a,b) and corrected (c,d).

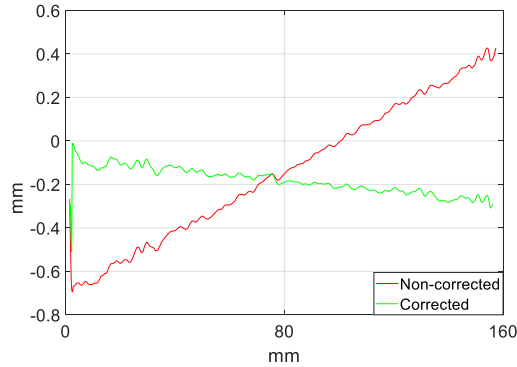
Additionally, Figure 5 shows the displacement profiles corresponding to the discontinuous lines in Figure 4. Red lines represent non-corrected values and green lines corrected displacements. As observed (Figures 4 and 5), the correction performed for the displacements in-plane indicates that both the displacements in  $-x$  and  $-y$  in the non-magnified and magnified images present a neglected value in the studied profile of the rigid body. Therefore, FP + 2D-DIC and PBMM integration do not generate distortions on the displacement maps.



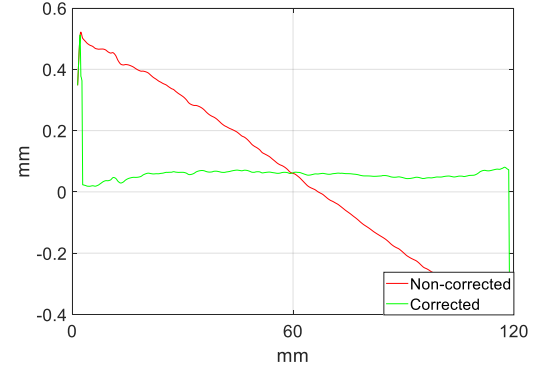
(a) Correction in  $-x$  without magnification



(b) Correction in  $-y$  without magnification



(c) Correction in  $-x$  with magnification  $\times 1.5$

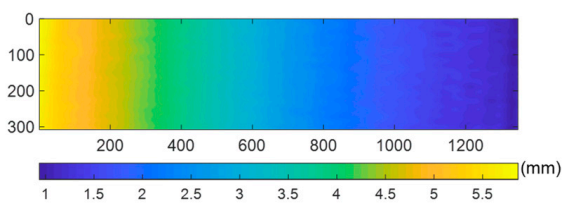


(d) Correction in  $-y$  with magnification  $\times 1.5$

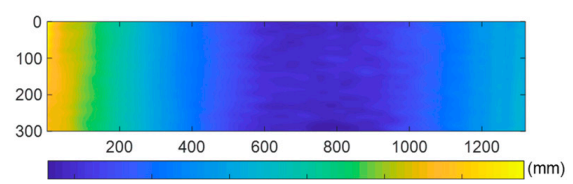
**Figure 5.** Correction profiles without magnification (a,b) and magnified  $\times 1.5$  (c,d).

4.2. Operational Deflection Shapes Test

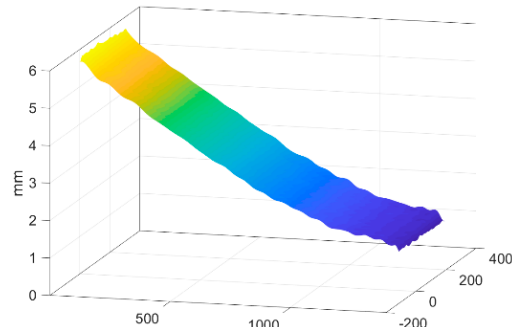
The operational deflection shapes associated to the analyzed frequencies in the second test are shown in Figure 6 (first and second natural frequency) and Figure 7a–c (third frequency).



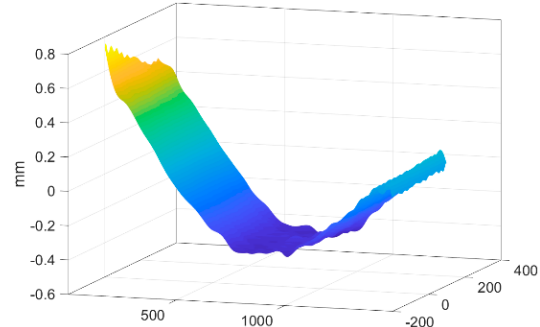
(a) Displacement map for first mode (20 Hz)



(b) Displacement map for second mode (160 Hz)



(c) Modal shape during first mode



(c) Modal shape during second mode

**Figure 6.** Modal shapes for the first and second vibration modes.

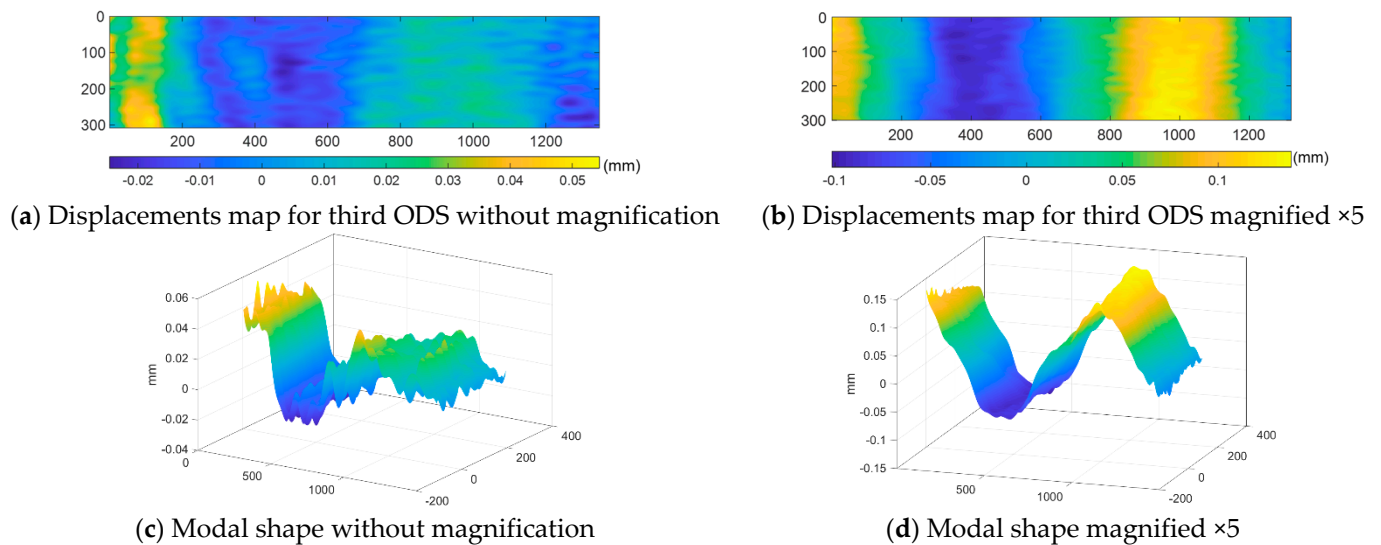


**Figure 7.** Comparison of maps displacement and mode shapes before and after magnifying.

The first and second ODSs are correctly interpreted without the requirement of PBMM as presented in Figure 6. However, it was not possible to adequately represent the third mode as shown in Figure 7a–c. Thus, for the third ODS, PBMM at  $5 \times$  factor was applied to achieve a clear representation of its modal shape. The ODSs maps obtained with and without applying PBMM are shown in Figure 7a,b. In addition, in Figure 7c,d the modal shapes are illustrated in 3D.

As depicted in Figure 7b, the displacements are scaled to the maximum and minimum value in order to illustrate how the noise was reduced after the application of Motion Magnification. Thus, the effectiveness of the combination of PMM and the FP + 2D-DIC technique is demonstrated for measuring displacements at high frequencies.

## 5. Conclusions

In this study, the potential of the combination of FP + 2D-DIC technique and phase-based Motion Magnification has been presented. After the application of the FP + 2D-DIC technique, the correct interpretation of the first and second vibration modes was verified. However, this technique was not conclusive for the third ODS. In this situation, Phase Based Motion Magnification demonstrated to be useful, obtaining remarkable results by observing the representation and measurement of displacements that occurred in the third modal shape.

In order to justify the use of the application of this combination, the method has been validated through the test of a rigid body presenting positive results, which indicates that the Magnification methodology can be used successfully together with FP + 2D-DIC in order to analyze more complex shape elements. In this way, as the main advantage, it can be established that the system would allow the best interpretation of modal shapes. This expands the field of application of the FP + 2D-DIC technique and offers a powerful low-cost tool with great potential in the industry. In fact, it facilitates, for instance, the obtaining of Operational Deflection Shapes in vibration testing on industrial components for automotive and aeronautic sectors, among others. It also reinforces FP + 2D-DIC as an interesting alternative for 3D-DIC. The main disadvantage of the integration of FP + 2D-DIC with PBMM is that quantification of displacements could require additional future analysis.

**Author Contributions:** Conceptualization, Á.M.-V., L.F.-S. and E.L.-A.; methodology, Á.M.-V., M.P.-C. and L.F.-S.; software, Á.M.-V., M.P.-C. and L.F.-S.; validation, Á.M.-V., M.P.-C. and L.F.-S.; formal analysis, Á.M.-V., M.P.-C. and L.F.-S.; investigation, Á.M.-V., M.P.-C. and L.F.-S.; resources, F.D.-G., L.F.-S. and E.L.-A.; data curation, Á.M.-V., M.P.-C. and L.F.-S.; writing—original draft preparation, M.P.-C.; writing—review and editing, Á.M.-V., M.P.-C. and L.F.-S.; visualization, Á.M.-V., M.P.-C. and L.F.-S.; supervision, Á.M.-V. and L.F.-S.; project administration, L.F.-S. and E.L.-A.; funding acquisition, F.D.-G., L.F.-S. and E.L.-A.; All authors have read and agreed to the published version of the manuscript.

**Funding:** This research was funded by University of Jaén and Andalusian Government through Programa Operativo FEDER Andalucía 2014–2020, grant number Ref. 1263076.

**Institutional Review Board Statement:** Not applicable.

**Informed Consent Statement:** Not applicable.

**Data Availability Statement:** Not applicable.

**Conflicts of Interest:** The authors declare no conflict of interest.

## References

- Sutton, M.A.; Orteu, J.J.; Schreier, H. *Image Correlation for Shape, Motion and Deformation Measurements-Basic Concepts, Theory and Applications*; Springer Science & Business Media: New York, NY, USA, 2009; p. 341.
- Takeda, M.; Mutoh, K. Fourier transform profilometry for the automatic measurement of 3-D object shapes. *Appl. Opt.* **1983**, *22*, 3977–3982. [[CrossRef](#)] [[PubMed](#)]
- Gorthi, S.S.; Rastogi, P. Fringe projection techniques: Whither we are? *Opt. Lasers Eng.* **2009**, *48*, 133–140. [[CrossRef](#)]
- Kinugasa, T.; Sakaguchi, T.; Gu, X.; Reinecker, H.C. Development and Assessment of a Single-Image Fringe Projection Method for Dynamic Applications. *Exp. Mech.* **2001**, *41*, 205–217.
- Ortiz, M.H. Location and Shape Measurement Using a Portable Fringe Projection System. *Exp. Mech.* **2005**, *45*, 197–204. [[CrossRef](#)]
- Rodríguez-Vera, R.; Avila, A.; Rayas, J.A.; Mendoza-Santoyo, F. Determination of Mechanical Vibration Properties of One-Dimensional Structures Using a Fringe Projection Method. In Proceedings of the Pacific Rim Conference on Lasers and Electro-Optics (CLEO—Technical Digest), Tokyo, Japan, 11–15 July 2005.
- Fu, Y. Low-frequency vibration measurement by temporal analysis of projected fringe patterns. *Opt. Lasers Eng.* **2010**, *48*, 226–234. [[CrossRef](#)]
- Barrientos, B.; Moreno, D.; Cywiak, M.; Pérez-López, C.; Mendoza-Santoyo, F. Vibration Analysis of a Metal Plate by Using Laser Vibrometry and Fringe Projection. In Proceedings of the Fifth Symposium Optics in Industry, Santiago De Queretaro, Mexico, 8 September 2005.
- Malesa, M.; Szczepanek, D.; Kujawińska, M.; Świercz, A.; Kołakowski, P. Monitoring of Civil Engineering Structures Using Digital Image Correlation Technique. In Proceedings of the EPJ Web of Conferences, Poitiers, France, 4–9 July 2010.
- Malowany, K.; Piekarczyk, A.; Malesa, M.; Kujawińska, M.; Więch, P. Application of 3D Digital Image Correlation for Development and Validation of FEM Model of Self-Supporting Arch Structures. *Appl. Sci.* **2019**, *9*, 1305. [[CrossRef](#)]
- Molina-Viedma, J.; López-Alba, E.; Felipe-Sesé, L.; Díaz, F.A. Modal Identification in an Automotive Multi-Component System Using HS 3D-DIC. *Materials* **2018**, *11*, 241. [[CrossRef](#)] [[PubMed](#)]
- Molina-Viedma, J.; López-Alba, E.; Felipe-Sesé, L.; Díaz, F.A.; Rodríguez-Ahlquist, J.; Iglesias-Vallejo, M. Modal Parameters Evaluation in a Full-Scale Aircraft Demonstrator under Different Environmental Conditions Using HS 3D-DIC. *Materials* **2018**, *11*, 230. [[CrossRef](#)] [[PubMed](#)]
- Felipe-Sesé, L.; Siegmann, P.; Díaz, F.A.; Patterson, E.A. Simultaneous in-and-out-of-plane displacement measurements using fringe projection and digital image correlation. *Opt. Lasers Eng.* **2014**, *52*, 66–74. [[CrossRef](#)]
- Felipe-Sesé, L.; Siegmann, P.; Díaz, F.A.; Patterson, E.A. Integrating fringe projection and digital image correlation for high-quality measurements of shape changes. *Opt. Eng.* **2014**, *53*, 44106. [[CrossRef](#)]
- Felipe-Sesé, L.; Díaz, F.A. Damage methodology approach on a composite panel based on a combination of Fringe Projection and 2D Digital Image Correlation. *Mech. Syst. Signal Process.* **2018**, *101*, 467–479. [[CrossRef](#)]
- Felipe-Sesé, L.; Garrido, F.A.D.; Patterson, E.A. Exploiting measurement-based validation for a high-fidelity model of dynamic indentation of a hyperelastic material. *Int. J. Solids Struct.* **2016**, *97–98*, 520–529. [[CrossRef](#)]
- Siegmann, P.; Álvarez-Fernández, V.; Díaz-Garrido, F.; Patterson, E.A. A simultaneous in- and out-of-plane displacement measurement method. *Opt. Lett.* **2010**, *36*, 10–12. [[CrossRef](#)]
- Wadhwa, N.; Rubinstein, M.; Durand, F.; Freeman, W.T. Phase-based video motion processing. *ACM Trans. Graph.* **2013**, *32*, 1–10. [[CrossRef](#)]
- Molina-Viedma, A.; Felipe-Sesé, L.; López-Alba, E.; Díaz, F. 3D mode shapes characterisation using phase-based motion magnification in large structures using stereoscopic DIC. *Mech. Syst. Signal Process.* **2018**, *108*, 140–155. [[CrossRef](#)]

20. Pan, B.; Yu, L.; Zhang, Q. Review of single-camera stereo-digital image correlation techniques for full-field 3D shape and deformation measurement. *Sci. China Technol. Sci.* **2017**, *61*, 2–20. [[CrossRef](#)]
21. Heredia-Ortiz, M.; Patterson, E.A. On the Industrial Applications of Moiré and Fringe Projection Techniques. *Strain* **2003**, *39*, 95–100. [[CrossRef](#)]
22. Takeda, M.; Ina, H.; Kobayashi, S. Fourier-transform method of fringe-pattern analysis for computer-based topography and interferometry. *J. Opt. Soc. Am.* **1982**, *72*, 156. [[CrossRef](#)]
23. Ghiglia, D.C.; Pritt, M.D. *Two-Dimensional Phase Unwrapping: Theory, Algorithms, and Software*; Wiley: Hoboken, NJ, USA, 1998.
24. Siegmann, P.; Felipe-Sese, L.; Diaz-Garrido, F. Improved 3D displacement measurements method and calibration of a combined fringe projection and 2D-DIC system. *Opt. Lasers Eng.* **2016**, *88*, 255–264. [[CrossRef](#)]